

Check for updates

Original Article



Longitudinal and lateral control of truck platoons based on finite-time sliding mode

Proc IMechE Part D:

J Automobile Engineering
1-18

© IMechE 2025

Article reuse guidelines:
sagepub.com/journals-permissions
DOI: 10.1177/09544070241309401
journals.sagepub.com/home/pid

Shuyou Yu^{1,2}, Shaoyu Sun¹, Boqun Zhang¹, Hong Chen³, Yongfu Li² and Baojun Lin¹

Abstract

In recent years, truck platooning has emerged as a promising technology to improve fuel efficiency, traffic flow, and road safety. However, achieving coordinated control of truck platoons presents significant challenges, especially considering the nonlinear dynamics and complex interactions between trucks. Longitudinal and lateral control of truck platoons with nonlinear dynamics are considered in this paper, in which a distributed controllers are designed. The characteristics of truck with nonlinear dynamics are considered, that is, a five-degree-of-freedom dynamics model of truck and tire model of "Magic Formula" are introduced, respectively. Simultaneously, a second-order longitudinal platoon model and a lateral lane-keeping model are developed, and a modified constant spacing policy to guarantee string stability is proposed. Then, a longitudinal and lateral decoupling sliding mode controller with finite-time convergence of truck platoons is designed. Furthermore, the finite-time stability and string stability of truck platoons are proved, respectively. Co-simulation experiments are carried out on the joint platform of Trucksim and Simulink, which demonstrate that the proposed controller can achieve fast attenuation of longitudinal and lateral errors, and consensus of truck platoons. Moreover, in order to guarantee safety of truck platoons, this paper gives a systematic estimation on the maximum driving velocity of truck platoons under different scenarios described by road curvatures and road adhesion coefficients. Finally, the main reason of instability for truck platoons is discussed.

Keywords

Truck platoon, longitudinal and lateral motion decoupling, sliding mode control, finite-time stability, string stability

Date received: 19 May 2024; accepted: 12 November 2024

Introduction

Control of truck platoons originates from the study of collaborative problems of multi-agent systems, in which truck platoons have advantages of reducing fuel consumption, eliminating truck collision risk, and improving road capacity. The control contents of truck platoons mainly include longitudinal control and lateral control. The longitudinal control of truck platoons serves to maintain a safe distance between trucks, thereby reducing the incidence of rear-end accidents and effectively saving fuel. Moreover, the lateral control of truck platoons ensures that trucks remain on a predetermined path and within the boundaries of the road. Since a truck is a nonlinear system considering coupling of lateral and longitudinal dynamics, and tire nonlinearity,2 it is a challenging problem to design effective longitudinal and lateral controllers of truck platoons.

The control objective of longitudinal control of truck platoons is to guarantee the consensus, that is, each truck in the platoon has the same velocity and the desired spacing,³ while guaranteeing the string stability. The single integrator model is the simplest models used to describe the longitudinal dynamics of a truck, in which the longitudinal position and velocity of a truck

Corresponding author:

Baojun Lin, College of Communication Engineering, Jilin University, No. 5988, Renmin Street, Changchun 130012, China. Email: linbj@jlu.edu.cn

¹College of Communication Engineering, Jilin University, Changchun,

²The Key Laboratory of Industrial Internet of Things and Networked Control, Chongqing University of Posts and Telecommunications, Chongqing, China

³College of Electronics and Information Engineering, Tongji University, Shanghai, China

are chosen as state and control input, respectively.⁴ Accordingly, the design of controller is transformed into a convex optimization problem based on the single integrator model, which can be solved efficiently.⁵ However, the single integrator model does not fit for analyzing string stability of platoons.⁶ Therefore, some theoretical results resort to the linear second-order model or third-order models. Based on linear secondorder models and the car-following (CF) theory, a sliding-mode control (SMC) strategy for a vehicle platoon is proposed in Peng et al. In Li et al., based on third-order kinematic models and the variable time headway (VTH) spacing policy, a longitudinal integral sliding mode (ISM) controller is designed to attenuate external disturbances. However, the nonlinear terms of a truck such as engines, transmissions, air resistance, and braking systems need to be considered. In Hu et al., based on nonlinear second-order model with air resistance, a sliding mode controller is proposed to incorporate observed disturbances for longitudinal cooperation of platoons. In Ali et al., ¹⁰ based on flatbed platoon towing model, a longitudinal proportionalintegral-derivative (PID) controller is designed to achieve vehicle platoon driving.

To some extent, string stability is the primary performance of a truck platoon.¹¹ In order to guarantee string stability, the spacing policy has to be considered as well. For example, in Rajamani, 12 autonomous control without wireless communication does not guarantee string stability under constant spacing (CS) policy. In Guo et al., 13 based on the constant time headway (CTH) policy, a distributed adaptive controller with a modified constant time headway policy is proposed to guarantee that spacing errors are uniformly ultimately bounded. In Guo et al., 14 an adaptive control method is proposed based on a quadratic spacing policy and nonlinear vehicle dynamics. Based on an improved time gap policy, a sliding mode controller with finite time disturbance observer (FTDO) is proposed in Chen et al., 15 which can guarantee strong string stability of the platoon. It is shown that a decentralized controller with a wireless communication can guarantee string stability of heterogeneous platoon based on a velocitydependent spacing policy.¹⁶

The objective of lateral control of truck platoons is to accurately track the centerline of desired reference path, while ensuring the safety and ride comfort of truck platoons. The Ackerman model¹⁷ is used to describe the lateral kinematic of a truck, in which the truck is represented as a bicycle. Based on the kinematic model, a distributed controller for a bus platoon is designed, in which a nonsingular integral terminal sliding mode (NITSM) and an adaptive integral reaching law are considered in Yu et al. 18 In Ali et al., 19 combining the kinematic model and dynamics model of a vehicle, a control strategy by using feedback linearization technique is proposed for vehicle platoon in an urban environment. In Dominguez et al.,²⁰ a lateral controller is proposed, in which comparison with three lateral controllers, such as Pure pursuit, Stanley, and a simplified kinematic steering controller is carried out.

Coupling characteristic is increasing significantly with increased acceleration, increased tire forces, or reduced road friction.²¹ Therefore, longitudinal and lateral dynamics need to be considered simultaneously. In Liu et al.,²² an improved hybrid genetic and adaptive particle swarm optimization (HGAPSO) algorithm is proposed to optimize the deformed wheels' trajectory. In Guo et al..²³ a hierarchical architecture used for coordinated longitudinal and lateral motion is proposed for four wheel drive (4WD) vehicles, which is composed of a global cooperative control layer, a control allocation layer, and an execution layer. In Feng et al.,²⁴ to deal with the uncertain interaction topology and external disturbances, a coordinated control scheme is proposed for a nonlinear heterogeneous platoon. In Shi et al.,²⁵ based on five-degree-of-freedom nonlinear dynamics model, a distributed PID controller is proposed for vehicle platoons, where the impact of tire nonlinearity of vehicle platoon under high-speed condition is analyzed.

Although fast consensus is an important performance of a truck platoon, most of researches can only obtain asymptotical consensus.²⁶ Note that, in general, finite-time convergence has properties of fast convergence and strong disturbance attenuation.²⁷ A finite-time sliding mode controller (FSMC) is proposed in Kwon and Chwa,²⁸ which can only guarantee to reach the sliding mode surface in finite time, but not reach the origin in finite time. In Yu et al.,²⁹ to reduce online computational burden, the nonlinear model of platoons is transformed into a global linear model based on the Koopman operator theory, where velocity tracking of vehicle with data-driven based model predictive control (MPC) is proposed.

In conclusion, the MPC algorithm requires accurate system models to achieve optimal performance, whereas the PID algorithm, while simpler, tends to be less robust. However, the finite time sliding mode control method offers several advantages, including finite time convergence, robustness, and reduced dependence on model accuracy. Aiming at fast convergence of errors of truck platoon, this paper proposes a distributed longitudinal and lateral control strategy based on the finite-time sliding mode control. The main manages of this paper are summarized as follows.

- (1) This paper applies a five-degree-of-freedom non-linear dynamics model of a truck and a "Magic Formula" tire model, which can accurately reflect the longitudinal-lateral motion of a truck and the nonlinear characteristics of tires compared to the kinematic model. Simultaneously, a second-order longitudinal platoon model and a lateral lane-keeping model are introduced. Furthermore, a modified constant spacing (MCS) policy to guarantee string stability is proposed.
- (2) A longitudinal and lateral decoupling control strategy of truck platoons is proposed, and finite-

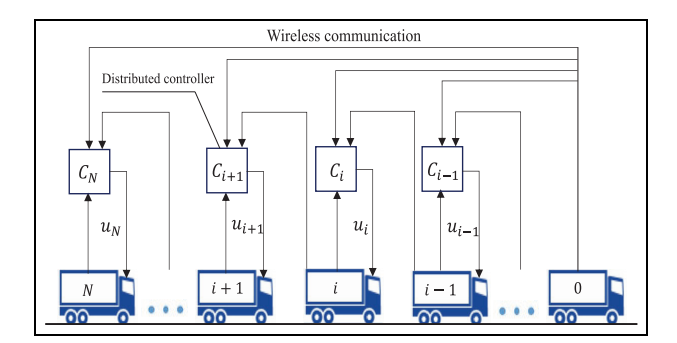


Figure 1. The distributed control framework of truck platoon.

time consensus, robustness, and string stability of truck platoons are proved.

(3) The effectiveness of the controller proposed is tested by the Trucksim/Simulink co-simulation. Moreover, in order to guarantee safety of truck platoons, a systematic estimation on the maximum driving velocities of truck platoons under different working conditions described by road curvatures and road adhesion coefficients is given, and the main reason of platoon instability is analyzed by simulation results.

The rest of the paper is organized as follows. In section "Problem setup," a detailed description of truck model, longitudinal and lateral platoon model are provided. In section "Distributed controller of truck platoon," a longitudinal and lateral sliding mode controllers are provided. In section "Properties of truck platoons," finite-time consensus and string stability of truck platoons are analyzed. In Section "Simulation experiments," simulation experiments for the control strategy proposed under different scenarios are provided. Finally, conclusions are drawn in Section "Conclusion."

Problem setup

Considering a truck platoon consisting of N+1 homogeneous trucks, where the leading truck is denoted by 0 and the following trucks are 1,2...N, respectively. Suppose that the leading truck is driven by a human driver along the desired path. The structure of the truck platoon is shown in Figure 1, in which a distributed control scheme is adopted. The motion of the truck platoon can be decoupled into a longitudinal motion and a lateral motion. The purpose of this paper is to design a distributed longitudinal and lateral controller for the following trucks to ensure longitudinal and lateral motion steadily, and to guarantee string stability. The required symbols for the truck platoon system are shown in Table 1.

Five-degree-of-freedom dynamics model of trucks

The five-degree-of-freedom dynamics model of trucks established in this paper,³⁰ shown in Figure 2, which

Table 1. Symbol for truck platoon system.

Symbol	Description		
Xi	Position of the <i>ith</i> vehicle		
$V_{x,i}$	Longitudinal velocity of the ith vehicle		
$V_{y,i}$	Lateral velocity of the ith vehicle		
$a_{x,i}$	Longitudinal acceleration of the ith vehicle		
ω_i	The yaw angle rate		
$e_{x,i}$	Longitudinal position error of the ith vehicle		
$e_{v,i}$	The velocity error of the ith vehicle		
$e_{y,i}$	Lateral position error of the ith vehicle		
l _z	The inertia moment around the z-axis		
a	The distances from front axle to mass center		
Ь	The distances from rear axle to mass center		
R	The wheel rolling radius		

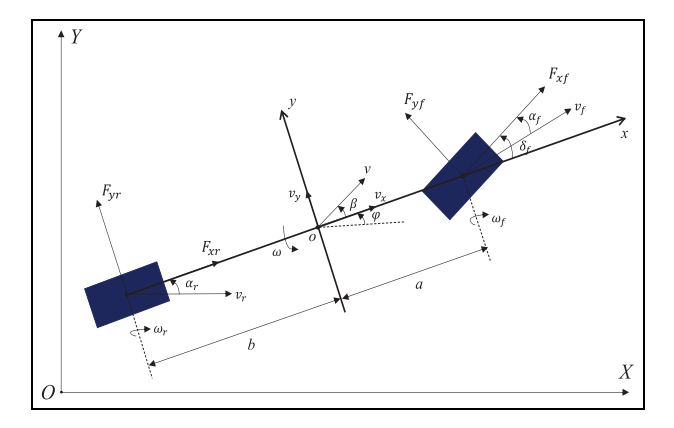


Figure 2. Five-degree-of-freedom dynamics model of truck.

assumes that the left and right wheel angles are the same, and there is no front and rear load deflection. The model characterizes the longitudinal motion, lateral motion, yawing motion, and front and rear wheel rotation of trucks. The trucks used in this paper are two-axle trucks. Only stability for the truck planar motion is considered in this paper, that is, both the roll and pitch motions are ignored.³⁰

According to Newton's Second Law, the five-degreeof-freedom dynamics model of trucks can be expressed as follows

$$\begin{cases} \dot{v}_{x} = \frac{1}{m} \left(F_{xf} \cos \delta_{f} - F_{yf} \sin \delta_{f} + F_{xr} - F_{wx} \right) + v_{y} \omega \\ \dot{v}_{y} = \frac{1}{m} \left(F_{xf} \sin \delta_{f} + F_{yf} \cos \delta_{f} + F_{yr} - F_{wy} \right) - v_{x} \omega \\ \dot{\omega} = \frac{1}{I_{z}} \left(aF_{xf} \sin \delta_{f} + aF_{yf} \cos \delta_{f} - bF_{yr} \right) \\ \dot{\omega}_{f} = \frac{1}{J_{f}} \left(T_{df} - RF_{xf} \right) \\ \dot{\omega}_{r} = \frac{1}{J_{r}} \left(T_{dr} - RF_{xr} \right) \end{cases}$$

$$(1)$$

where v_x , v_y , and ω are the longitudinal velocity, lateral velocity, yaw angle rate of truck. The terms of ω_f and ω_r are the angular velocity of front and rear wheels; m

is the total mass of truck; I_z is the moment of inertia around yaw axis; a and b are the distances from front axle and rear axle to mass center; J_f and J_r are the moment of inertia of front and rear wheel; δ_f is the lateral control input representing steering angle of the front wheel; T_{df} and T_{dr} are the longitudinal control input representing the torque of front and rear wheel; F_{xf} , F_{xr} , F_{yf} , and F_{yr} are the longitudinal tire force of front wheel, longitudinal tire force of rear wheel, lateral tire force of front wheel, and lateral tire force of front wheel, respectively; R is the wheel rolling radius. Since the air resistance accounts for almost all of the driving resistance when a high-speed and fully loaded truck platoon is moving,³¹ this paper only considers the air resistance. The terms of F_{wx} and F_{wr} are the longitudinal and lateral air resistance as follows

$$\begin{cases} F_{wx} = \frac{1}{2} \operatorname{sgn}(v_x) \rho C_x A_x v_x^2 \\ F_{wy} = \frac{1}{2} \operatorname{sgn}(v_y) \rho C_y A_y v_y^2 \end{cases}$$
 (2)

where C_x and C_y are the longitudinal and lateral air resistance coefficients; A_x and A_y are the longitudinal and lateral windward areas of truck; ρ is the air density. Since the direction of air resistance is always opposite to the direction of travel of truck, sign function is introduced into the model to describe the air resistance acting on a moving truck.

"Magic Formula" tire model

Since the nonlinear characteristics of tires has a greater impact on the stability of vehicle platoon at high speeds, ²⁵ a nonlinear model of tires needs to be taken into account. The "Magic Formula" tire model is applied in this paper, ³² in which the tire forces are calculated by

$$\begin{cases} F_{xf0} = D\sin\left(C\arctan\left(Bk_f - E\left(Bk_f - \arctan Bk_f\right)\right)\right) \\ F_{xr0} = D\sin\left(C\arctan\left(Bk_r - E\left(Bk_r - \arctan Bk_r\right)\right)\right) \\ F_{yf0} = D\sin\left(C\arctan\left(B\alpha_f - E\left(B\alpha_f - \arctan B\alpha_f\right)\right)\right) \\ F_{yr0} = D\sin\left(C\arctan\left(B\alpha_r - E\left(B\alpha_r - \arctan B\alpha_r\right)\right)\right) \end{cases}$$

where k_f , k_r , α_f , and α_r are slip ratios and slip angles of front and rear tires; F_{xf0} , F_{xr0} , F_{yf0} , and F_{yr0} are the longitudinal tire force of front wheel, longitudinal tire force of rear wheel, lateral tire force of front wheel, and lateral tire force of front wheel in the steady state, respectively; B, C, D, and E are the parameters of tires.

Remark 1. The parameters of tires in the "Magic Formula" are fitting parameters, which need to be obtained by means of curve fitting. Furthermore, the specific values of tire parameters are different under different road adhesion coefficients, vertical loads and

wheel camber angles.³² The road adhesion coefficient selected for the fitting of this paper is 0.85 as the wheel camber angles is 0 degree.³³

The slip angles of front and rear tires can be calculated as

$$\begin{cases} \alpha_f = \delta_f - \arctan\left(\frac{v_y + a\omega}{v_x}\right) \\ \alpha_r = -\arctan\left(\frac{v_y - b\omega}{v_x}\right) \end{cases}$$
 (4)

The slip ratios of front and rear tires can be calculated as

$$\begin{cases} k_f = \frac{\omega_f R - v_{\omega x}}{|v_{\omega x}|} \\ k_r = \frac{\omega_r R - v_{\omega x}}{|v_{\omega x}|} \end{cases}$$
 (5)

Since the longitudinal and lateral tire forces affect each other, tire of combined slip is taken into account.³⁴ The tire forces can be calculated by

$$\begin{cases}
F_{xf} = F_{xf0} \cdot \cos(\arctan(B_{gxf}(\alpha) \cdot \alpha_f)) \\
F_{yf} = F_{yf0} \cdot \cos(\arctan(B_{gyf}(k) \cdot k_f)) \\
F_{xr} = F_{xr0} \cdot \cos(\arctan(B_{gxr}(\alpha) \cdot \alpha_r)) \\
F_{yr} = F_{yr0} \cdot \cos(\arctan(B_{gyr}(k) \cdot k_r)) \\
B_{gxf}(\alpha) = r_{x1} \cdot \cos(\arctan(r_{x2} \cdot k_f)) \\
B_{gxr}(\alpha) = r_{x1} \cdot \cos(\arctan(r_{x2} \cdot k_r)) \\
B_{gyf}(k) = r_{y1} \cdot \cos(\arctan(r_{y2} \cdot \alpha_f)) \\
B_{gyr}(k) = r_{y1} \cdot \cos(\arctan(r_{y2} \cdot \alpha_r))
\end{cases}$$
(6)

where $B_{gxf}(\alpha)$, $B_{gxr}(\alpha)$, $B_{gyf}(k)$, and $B_{gyr}(k)$ are the longitudinal and lateral shape functions of tire slip; terms of α and k are the inputs of the longitudinal and lateral shape functions of tire slip, respectively; r_{x1} , r_{x2} , r_{y1} , and r_{y2} are the longitudinal slip coefficients and lateral slip coefficients.

Longitudinal error model of truck platoon

This section establishes longitudinal and lateral platoon models by using Vehicle-to-Everything (V2X) wireless communication technology, which allows to obtain the information of nearby trucks and road. The predecessor-leader following (PLF) information flow topology is adopted in this paper.³⁵

As shown in Figure 3, suppose that the leading truck is driven by a human driver along the desired path. Its longitudinal position and longitudinal velocity are given as $x_0(t)$ and $v_{x,0}(t)$ a priori. For each following truck i, $i \in 1, 2...N$, describe its longitudinal position and longitudinal velocity as $x_i(t)$ and $v_{x,i}(t)$. In order to improve the capacity of the road and guarantee string

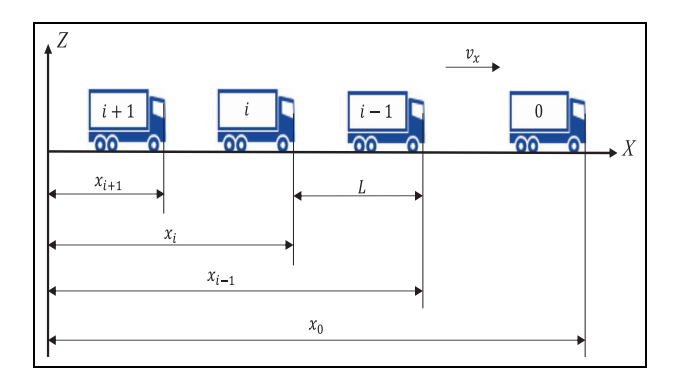


Figure 3. The longitudinal spacing error model of truck platoon.

stability, a modified constant spacing (MCS) policy is proposed in this paper.

Define L as the desired spacing containing the length of a truck. The longitudinal spacing error between the ith following truck and leading truck is defined as

$$e_{i,0}(t) = x_i(t) - (x_0(t) - iL) \tag{7}$$

The longitudinal spacing error between the *i*th following truck and the (i-1)th following truck is

$$e_i(t) = x_i(t) - (x_{i-1}(t) - L)$$
 (8)

In terms of (7) and (8), one has

$$e_{i,0}(t) = e_1(t) + e_2(t) + e_3(t)... + e_i(t)$$
 (9)

Define the integrated longitudinal spacing error of the *i*th following truck as

$$e_{x,i}(t) = \sigma_1 e_{i,0}(t) + \sigma_2 e_i(t)$$
 (10)

where σ_1 and σ_1 are positive constant parameters, and $\sigma_1 + \sigma_2 = 1$.

Remark 2. Only spacing policy of (7) is used, the number of vehicles in a platoon is unlimited, but collisions might occur in the case of velocity reduction. Only spacing policy of (8) is used, collisions can be avoided, but string stability will not be guaranteed due to errors accumulation when the number of vehicles is increased.³⁵

The derivative of (10) is

$$\begin{cases} \dot{e}_{x,i}(t) = v_{x,i}(t) - \sigma_1 v_{x,0}(t) - \sigma_2 v_{x,i-1}(t) \\ \ddot{e}_{x,i}(t) = a_{x,i}(t) - \sigma_1 a_{x,0}(t) - \sigma_2 a_{x,i-1}(t) \end{cases}$$
(11)

where $a_{x,i}(t)$ and $a_{x,0}(t)$ are longitudinal acceleration of the *i*th following truck and leading truck.

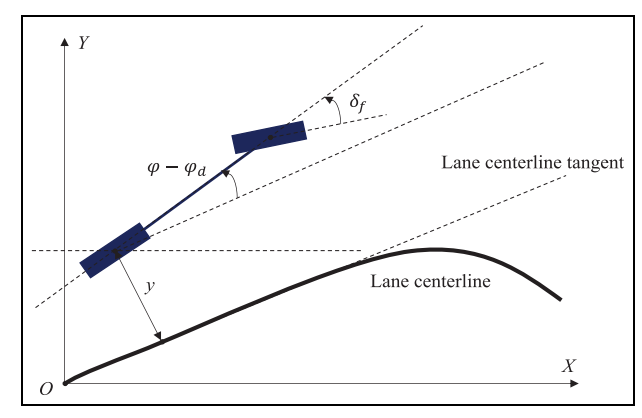


Figure 4. The lane-keeping model of truck platoon.

Let the longitudinal intermediate control inputs as $u_{x,i}(t) = a_{x,i}(t)$, and let the longitudinal velocity error of the *i*th following truck as $e_{v,i}(t) = \dot{e}_{x,i}(t)$. Therefore, the longitudinal error model of truck platoon can be described as

$$\begin{cases} \dot{e}_{x,i}(t) = e_{v,i}(t) \\ \dot{e}_{v,i}(t) = f_{x,i}(t) + u_{x,i}(t) + d_{x,i}(t) \end{cases}$$
(12)

where $f_{x,i}(t) = -\sigma_1 a_{x,0}(t) - \sigma_2 a_{x,i-1}(t)$ denotes the term that does not contain $u_{x,i}(t)$; $d_{x,i}(t)$ denotes the longitudinal unknown but bounded disturbances.

Lane-keeping model of truck platoon

In this section, a lane-keeping model of the truck platoon is established. As shown in Figure 4, suppose that leading truck is driven by a human along the centerline of the lane, and following trucks keep moving by obtaining information of error of the current lateral position to the centerline of lane and angular error of the travel direction to the tangential direction of the centerline of the lane.

Define an integrated lateral position error for the *i*th following truck in the platoon as

$$e_{v,i}(t) = \sigma_3 y_i(t) + \sigma_4 \parallel \left(\varphi_i(t) - \varphi_{d,i}(t) \right) \parallel \tag{13}$$

where $y_i(t)$ is the lateral position of the *i*th following truck; $\varphi_i(t)$ and $\varphi_{d,i}(t)$ are actual yaw angle and desired yaw angles of the *i*th following truck; σ_3 and σ_4 are positive constant parameters.

The derivative of (13) is

$$\begin{cases}
\dot{e}_{y,i}(t) = \sigma_3 v_{y,i}(t) + \sigma_4 \parallel (\omega_i(t) - \omega_{d,i}(t)) \parallel \\
\ddot{e}_{y,i}(t) = \sigma_3 a_{y,i}(t) + \sigma_4 \parallel (\dot{\omega}_i(t) - \dot{\omega}_{d,i}(t)) \parallel
\end{cases}$$
(14)

where $v_{y,i}(t)$ and $a_{y,i}(t)$ are the lateral velocity and lateral acceleration of the *i*th following truck; $\omega_i(t)$, $\dot{\omega}_i(t)$, $\omega_{d,i}(t) = Kv_{x,i}(t)$, and $\dot{\omega}_{d,i}(t) = 0$ are the yaw angle rate, yaw angle acceleration, desired yaw angle rate,

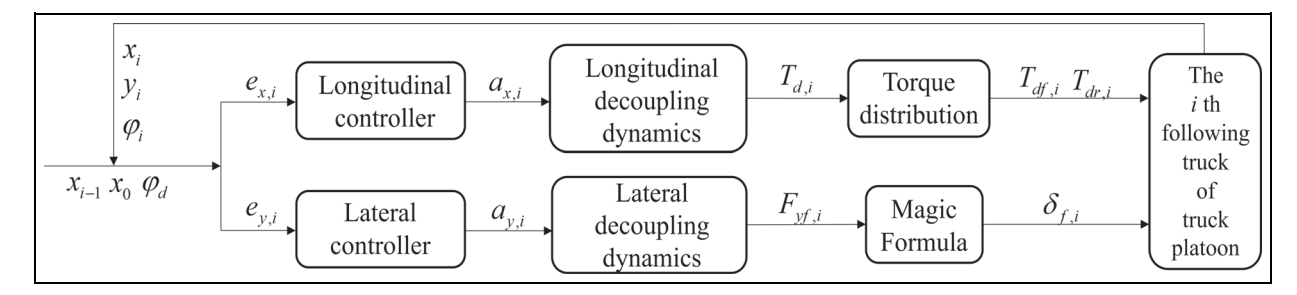


Figure 5. The structure with longitudinal and lateral decoupling control.

and desired yaw angle acceleration of the *i*th following truck; *K* is road curvature.

Let the lateral intermediate control inputs as $u_{u,i}(t) = a_{y,i}(t)$, and let the lateral velocity error of the *i*th following truck as $e_{d,i}(t) = \dot{e}_{y,i}(t)$. Therefore, the lateral lane-keeping model of truck platoon can be described as

$$\begin{cases} \dot{e}_{y,i}(t) = e_{d,i}(t) \\ \dot{e}_{d,i}(t) = f_{y,i}(t) + \sigma_3 u_{y,i}(t) + d_{y,i}(t) \end{cases}$$
(15)

where $f_{y,i}(t) = \sigma_4 \parallel (\omega_i(t) - \dot{\omega}_{d,i}(t)) \parallel$ denotes the term that does not contain $u_{y,i}(t)$; $d_{y,i}(t)$ denotes the lateral unknown but bounded disturbances.

Control objective of truck platoon

In order to ensure longitudinal and lateral motion of truck platoon steadily, control objectives are described as follows.

(1) Longitudinal finite-time consensus: When a truck platoon move smoothly, the integrated longitudinal spacing error and the longitudinal velocity error of the *i*th following truck should converge to zero in finite time $t_{x,i}$, that is

$$\begin{cases}
\lim_{t \to t_{x,i}} \| e_{x,i}(t) \| = 0 \\
\lim_{t \to t_{y,i}} \| e_{y,i}(t) \| = 0
\end{cases}$$
(16)

(2) Lateral finite-time stability: When a truck platoon moves smoothly along a curve, the *i*th following truck should keep moving along the centerline of the lane. According to Menzel et al., 36 the admissible lateral error is set to 0.5 m. In addition, the ride comfort and safety of truck platoons also need to be considered. The error of yaw angle rate of the *i*th following truck should be minimized in finite time $t_{y,i}$, that is

$$\begin{cases}
\lim_{t \to t_{y,i}} \parallel e_{y,i}(t) \parallel = 0 \\
\lim_{t \to t_{y,i}} \parallel \omega_i(t) - \omega_{d,i}(t) \parallel = 0
\end{cases}$$
(17)

(3) String stability³⁷: When a truck platoon is subject to unknown disturbances, the spacing errors are not amplified along the platoon, that is

$$\|G_{x,i}(s)\| = \|\frac{e_{x,i}(s)}{e_{x,i-1}(s)}\| \le 1$$
 (18)

where $G_{x,i}(s)$ denotes the transfer function of the longitudinal error; $e_{x,i}(s)$ and $e_{x,i-1}(s)$ denote the related Laplace transform of $e_{x,i}(t)$ and $e_{x,i-1}(t)$, respectively.

Distributed controller of truck platoon

This paper develops a longitudinal and lateral decoupling control strategy with guaranteed finite-time convergence, in which the longitudinal controller ensures that the truck platoon travel along the desired path, and the lateral controller ensures that the platoon does not cross the lane boundary. The structure with the longitudinal and lateral decoupling controller is shown in Figure 5.

Longitudinal controller

It is necessary to decouple longitudinal and lateral dynamics of trucks in order to design the decoupling controllers. Suppose that the steering angle of the front wheel is small, and the longitudinal dynamics model of the *i*th following truck can be formulated as

$$\dot{v}_{x,i}(t) = \frac{1}{m} \left(F_{xf,i}(t) + F_{xr,i}(t) - F_{wx,i}(t) \right) + v_{y,i}(t) \omega_i(t)$$
(19)

To guarantee finite-time convergence, the fast terminal sliding mode (FTSM) controller is designed, in which the longitudinal sliding mode surface of the *i*th following truck is

$$s_{x,i}(t) = \dot{e}_{x,i}(t) + c_1 e_{x,i}(t) + c_2 e_{x,i}^q(t)$$
 (20)

where c_1 and c_2 are positive constants; q is the ratio of two positive odd numbers, and 0 < q < 1.

In terms of (11), (12), and (20), the longitudinal acceleration of the *i*th following truck can be calculated as

$$u_{x,i}(t) = \sigma_1 a_{x,0}(t) + \sigma_2 a_{x,i-1}(t) - c_1 e_{v,i}(t) - c_2 q e_{x,i}^{q-1}(t) e_{v,i}(t) - k_1 s_{x,i}(t) - \eta_1 \operatorname{sgn}(s_{x,i}(t)) - D_{x,i}(t) \operatorname{sgn}(s_{x,i}(t))$$
(21)

where k_1 and η_1 are positive constants; $D_{x,i}(t)$ is the upper bound of the longitudinal unknown disturbance, that is, $|d_{x,i}(t)| \leq D_{x,i}(t)$.

In terms of (19) and (21), the desired total longitudinal tire force of the *i*th following is

$$F_{x,i,d}(t) = F_{xf,id}(t) + F_{xr,id}(t)$$

$$= m(\sigma_{1}a_{x,0}(t) + \sigma_{2}a_{x,i-1}(t) - c_{1}e_{v,i}(t))$$

$$- mc_{2}qe_{x,i}^{q-1}(t)e_{v,i}(t) - mk_{1}s_{x,i}(t)$$

$$- mv_{y,i}(t)\omega_{i}(t) + F_{wx,i}(t)$$

$$- m\eta_{1}\operatorname{sgn}(s_{x,i}(t)) - mD_{x,i}(t)\operatorname{sgn}(s_{x,i}(t))$$
(22)

Therefore, the desired total wheel torque of the *i*th following truck can be expressed as

$$T_{d,i,d}(t) = RF_{x,i,d}(t)$$
(23)

Remark 3. According to torque distribution principle,²⁵ the ratio of the desired front wheel torque $T_{df,i,d}(t)$ and the desired rear wheel torque $T_{dr,i,d}(t)$ is selected as 1:24.

Lateral controller

Accordingly, the lateral dynamics model of the *i*th following truck can be formulated as

$$\begin{cases}
\dot{v}_{y,i}(t) = \frac{1}{m} \left(F_{yf,i}(t) + F_{yr,i}(t) - F_{wy,i}(t) \right) - v_{x,i}(t) \omega_i(t) \\
\dot{\omega}_i(t) = \frac{1}{I_z} \left(a F_{yf,i}(t) - b F_{yr,i}(t) \right)
\end{cases}$$
(24)

Similarly, the lateral sliding mode surface of the *i*th following truck is expressed as

$$s_{y,i}(t) = \dot{e}_{y,i}(t) + c_3 e_{y,i}(t) + c_4 e_{y,i}^p(t)$$
 (25)

where c_3 and c_4 are positive constants; p is the ratio of two positive odd numbers, and 0 .

In terms of (14), (15), and (25), the lateral acceleration of the *i*th following truck can be calculated as

$$u_{y,i}(t) = -\frac{1}{\sigma_3} (\sigma_4 \| (\dot{\omega}_i(t) - \dot{\omega}_{d,i}(t)) \| + c_3 e_{d,i}(t))$$

$$-\frac{1}{\sigma_3} c_4 p e_{y,i}^{p-1}(t) e_{d,i}(t) - \frac{1}{\sigma_3} k_2 s_{y,i}(t)$$

$$-\frac{1}{\sigma_3} \eta_2 \operatorname{sgn}(s_{y,i}(t)) - D_{y,i}(t) \operatorname{sgn}(s_{y,i}(t))$$
(26)

where k_2 and η_2 are positive constants; $D_{y,i}(t)$ is the upper bound of the lateral disturbance, that is, $|d_{y,i}(t)| \leq D_{y,i}(t)$.

Remark 4. In order to avoid the chattering phenomenon caused by the discontinuity of the symbolic function sgn(s) of (21) and (26), the saturation function sat(s/c) will replace sgn(s) during the experiments, where c is a positive constant representing the thickness of the boundary of the sliding mode surface.

In terms of (24) and (26), the desired lateral tire force of front wheel of the *i*th following truck can be expressed as

$$F_{yf,i,d}(t) = P(-\sigma_4 \dot{\omega}_{d,i}(t) + c_3 e_{d,i}(t))$$

$$+ P(c_4 p e_{y,i}^{p-1}(t) e_{d,i}(t) + k_2 s_{y,i}(t))$$

$$+ P(\eta_2 \operatorname{sgn}(s_{y,i}(t)) + \sigma_3 D_{y,i}(t) \operatorname{sgn}(s_{y,i}(t)))$$

$$+ P\sigma_3 v_{x,i}(t) \omega_i(t) + Q F_{yr,i}(t) - R F_{wy,i}(t)$$

$$(27)$$

where

$$\begin{cases}
P = -\frac{mI_z}{\sigma_3 I_z + ma\sigma_4} \\
Q = \frac{\sigma_3 + b\sigma_4}{\sigma_3 I_z + ma\sigma_4} \\
R = \frac{\sigma_3 I_z}{\sigma_3 I_z + ma\sigma_4}
\end{cases} (28)$$

In terms of (3), (6), and (27), the desired slip angle of front tire of the *i*th following truck can be calculated as

$$\alpha_{f,i,d}(t) = \Pi^{-1}(F_{yf,i,d}(t))$$
 (29)

where Π^{-1} represents the inverse function of the "Magic Formula".³²

Remark 5. According to the tire characteristic curve, ³⁸ when the desired lateral force is large enough, two desired slip angles can be calculated, however only the smaller one is chosen in this paper. ³²

Therefore, according to (4) and (29), the lateral control input of the truck platoon representing the desired

steering angle of the front wheel of the *i*th following truck be expressed as

$$\delta_{f,i,d}(t) = \alpha_{f,i,d}(t) + \arctan\left(\frac{v_{y,i}(t) + a\omega_i(t)}{v_{x,i}(t)}\right)$$
(30)

Properties of truck platoons

In this section, the properties of truck platoons, that is, consensus, string stability are investigated.

The following Lemma will be used in the proof of finite time consensus.

Lemma 1.³⁹ Consider the autonomous system

$$\Phi = \vartheta(\Phi), \Phi(0) = \Phi_0 \tag{31}$$

where $\vartheta \in \mathbb{R}^n \to \mathbb{R}^n$ is continuous on an open neighborhood of the origin $\Phi = 0$, and $\vartheta(0) = 0$.

Suppose there exists a continuous differentiable function $E: \mathbb{R}^n \to \mathbb{R}$, scalars λ , $\gamma > 0$, $\beta \in (0,1)$, and an open neighborhood M of the origin such that

$$\dot{E}(\Phi) \leqslant -\gamma E(\Phi) - \lambda E(\Phi)^{\beta} \tag{32}$$

For all $\Phi \in M \setminus \{0\}$, $E(\Phi) > 0$, and E(0) = 0. The origin of the system (31) is finite-time reachable, and the setting time T_s satisfies

$$T_s \leqslant \frac{1}{\gamma(1-\beta)} \ln\left(1 + \frac{\gamma}{\lambda} E(\Phi_0)^{1-\beta}\right) \tag{33}$$

Finite-time reachability

The reachability and robustness of a platoon with respect to unknown disturbances are analyzed

Theorem 1. The state of the longitudinal error model (12) of a truck platoon can reach its sliding mode surface (20) under the longitudinal controller (21) in finite time, and the setting time $t_{x,i}$ satisfies $t_{x,i} \leq \frac{1}{k_1} \ln\left(1 + \frac{\sqrt{2}k_1}{\eta_1} V_{x,i}(0)^{0.5}\right)$.

Proof 1. First, the longitudinal error model (12) of a truck platoon is

$$\begin{cases}
\dot{e}_{x,i}(t) = e_{y,i}(t) \\
\dot{e}_{y,i}(t) = f_{x,i}(t) + u_{x,i}(t) + d_{x,i}(t)
\end{cases}$$
(34)

Accordingly, the longitudinal sliding mode surface (20) is

$$s_{x,i}(t) = \dot{e}_{x,i}(t) + c_1 e_{x,i}(t) + c_2 e_{x,i}^q(t)$$
 (35)

The derivative of (35) is

$$\dot{s}_{x,i}(t) = f_{x,i}(t) + u_{x,i}(t) + d_{x,i}(t) + c_1 e_{y,i}(t) + c_2 q e_{x,i}^{q-1}(t) e_{y,i}(t)$$
(36)

In terms of (34), the longitudinal controller (21) can be rewritten as

$$u_{x,i}(t) = -f_{x,i}(t) - c_1 e_{v,i}(t) - c_2 q e_{x,i}^{q-1}(t) e_{v,i}(t) - k_1 s_{x,i}(t) - \eta_1 \operatorname{sgn}(s_{x,i}(t)) - D_{x,i}(t) \operatorname{sgn}(s_{x,i}(t))$$
(37)

Choosing $V_{x,i}(t) = 0.5s_{x,i}^2(t)$ as a candidate Lyapunov function, one has

$$\dot{V}_{x,i}(t) = s_{x,i}(t)\dot{s}_{x,i}(t)
= s_{x,i}(t)(f_{x,i}(t) + c_1e_{v,i}(t) + c_2qe_{x,i}^{q-1}(t)e_{v,i}(t))
+ s_{x,i}(t)(-f_{x,i}(t) - c_1e_{v,i}(t) - c_2qe_{x,i}^{q-1}(t)e_{v,i}(t))
+ s_{x,i}(t)(-k_1s_{x,i}(t) - \eta_1\operatorname{sgn}(s_{x,i}(t)))
+ s_{x,i}(t)(d_{x,i}(t) - D_{x,i}(t)\operatorname{sgn}(s_{x,i}(t)))$$
(38)

Equation (38) can be simplified as

$$\dot{V}_{x,i}(t) = -k_1 s_{x,i}^2(t) - \eta_1 |s_{x,i}(t)|
+ d_{x,i}(t) s_{x,i}(t) - D_{x,i}(t) |s_{x,i}(t)|$$
(39)

Since $d_{x,i}(t)s_{x,i}(t) \le |d_{x,i}(t)||s_{x,i}(t)|$ and $|d_{x,i}(t)| \le D_{x,i}(t)$, one has

$$\dot{V}_{x,i}(t) \leqslant -k_1 s_{x,i}^2(t) - \eta_1 |s_{x,i}(t)|
+ |d_{x,i}(t)| |s_{x,i}(t)| - D_{x,i}(t) |s_{x,i}(t)|
\leqslant -k_1 s_{x,i}^2(t) - \eta_1 |s_{x,i}(t)|$$
(40)

In terms of $V_{x,i}(t) = 0.5s_{x,i}^2(t)$, one has

$$\dot{V}_{x,i}(t) \leqslant -2k_1 V_{x,i}(t) - \sqrt{2} \eta_1 V_{x,i}(t)^{0.5}$$
(41)

Therefore, when $s_{x,i}(t) \neq 0$, $V_{x,i}(t) > 0$, $\dot{V}_{x,i}(t) < 0$. According to Lemma 1, when there is an unknown but bounded disturbance, the system state can reach its sliding mode surface under the longitudinal controller (21), and the setting time $t_{x,i}$ satisfies

$$t_{x,i} \le \frac{1}{k_1} \ln \left(1 + \frac{\sqrt{2}k_1}{\eta_1} V_{x,i}(0)^{0.5} \right)$$
 (42)

Theorem 2. The state of the lateral lane-keeping model (15) of a truck platoon can reach its sliding mode surface (25) under the lateral controller (26) in finite time, and the setting time $t_{y,i}$ satisfies $t_{y,i} \leq \frac{1}{k_2} \ln\left(1 + \frac{\sqrt{2}k_2}{\eta_2} V_{y,i}(0)^{0.5}\right)$.

Proof 2. Since the proof is similar to the proof of Theorem 1, it is omitted.

Finite-time consensus

The finite-time consensus of the truck platoon is analyzed.

Theorem 3. Denote $c_1 > 0$, $c_2 > 0$, and 0 < q < 1. When the state of the longitudinal error model (12) of a truck platoon reaches its sliding mode surface (20), it will converge to zero in finite time, that is, the longitudinal system of truck platoon is finite-time consensus.

Proof 3. When the state of system (12) state reaches its sliding mode surface (20), one has

$$\dot{e}_{x,i}(t) + c_1 e_{x,i}(t) + c_2 e_{x,i}^q(t) = 0 \tag{43}$$

Multiply both sides of (43) by $e_{x,i}^{-q}(t)$, one has

$$e_{x,i}^{-q}(t)\dot{e}_{x,i}(t) + c_1 e_{x,i}^{1-q}(t) = -c_2$$
(44)

Denote $m_i(t) = e_{x,i}^{1-q}(t)$, then

$$\frac{dm_i(t)}{dt} + (1 - q)c_1m_i(t) = -(1 - q)c_2 \tag{45}$$

When $e_{x,i}(t) = 0$, $m_i(t) = 0$. According to Lemma 1, the settling time $T_{x,i}$ from any initial state $e_{x,i(0)} \neq 0$ to zero is

$$T_{x,i} = \frac{1}{c_1(1-q)} \ln \left(\frac{c_1 e_{x,i}(0)^{1-q} + c_2}{c_2} \right)$$
 (46)

Since $c_1 > 0$, $c_2 > 0$, and 0 < q < 1, the longitudinal system of the truck platoon is finite-time consensus.

Theorem 4. Denote $c_3 > 0$, $c_4 > 0$, and 0 . When the state of the lateral lane-keeping (15) of a truck platoon reaches its sliding mode surface (25), it will converge to zero in finite time, that is, the lateral lane-keeping system of truck platoon is finite-time stability.

Proof 4. Since the proof is similar to the proof of Theorem 3, it is omitted.

String stability

Theorem 5. Denote $0 < \sigma_2 < 1$. The spacing errors are not amplified by propagating along the platoon, that is, the truck platoon is string stable.

Proof 5. When a truck platoon is in steady state, $e_{x,i}(t) = 0$ and $e_{x,i-1}(t) = 0$. According to (10), one has

$$\begin{cases} \sigma_1 e_{i,0}(t) + \sigma_2 e_i(t) = 0\\ \sigma_1 e_{i-1,0}(t) + \sigma_2 e_{i-1}(t) = 0 \end{cases}$$
(47)

where σ_1 and σ_2 are positive scalars, and $\sigma_1 + \sigma_2 = 1$.

Table 2. The truck parameters.

Parameters	Value	Parameters	Value	
m a J _f A _x C _x R L	18,000 kg 3.5 m 24 kg · m ² 6.8 m ² 0.6 0.51 m 20 m	I _z b J _r A _y C _y ρ	130,421 kg · m ² 1.5 m 48 kg · m ² 11.25 m ² 0.8 1.2258 kg/m ³	

In terms of (9), one has

$$\begin{cases}
e_{i,0}(t) = e_1(t) + e_2(t) + e_3(t) \dots + e_i(t) \\
e_{i-1,0}(t) = e_1(t) + e_2(t) + e_3(t) \dots + e_{i-1}(t)
\end{cases}$$
(48)

In terms of (47) and (48), one has

$$\begin{cases} e_{1}(t) + e_{2}(t) + e_{3}(t)... + e_{i-1}(t) + \left(1 + \frac{\sigma_{2}}{\sigma_{1}}\right)e_{i}(t) = 0\\ e_{i-1,0}(t) + \frac{\sigma_{2}}{\sigma_{1}}e_{i-1}(t) = 0 \end{cases}$$
(49)

By simplification of (49), one has

$$\left(1 + \frac{\sigma_2}{\sigma_1}\right) e_i(t) = \frac{\sigma_2}{\sigma_1} e_{i-1}(t) \tag{50}$$

Applying the Laplace transform to (50), one has

$$\|\frac{e_i(s)}{e_{i-1}(s)}\| = \|\frac{\sigma_2}{\sigma_1} \cdot \frac{\sigma_1}{\sigma_1 + \sigma_2}\| = \sigma_2$$
 (51)

Since $\sigma_1 > 0$, $\sigma_2 > 0$ and $\sigma_1 + \sigma_2 = 1$, $0 < \sigma_2 < 1$. Therefore, according to (18), the truck platoon is string stable.

Simulation experiments

In order to verify the effectiveness of the longitudinal and lateral controller proposed, co-simulation experiments are carried out based on Trucksim and Simulink in this section, in which a homogeneous truck platoon consisting of a leading truck and four following trucks is chosen in different scenarios. The control inputs of leading truck are provided a priori, and the control inputs of following trucks are obtained from the controller proposed. The parameters of trucks are listed in Table 2, the tire parameters are listed in Table 3, and the controller parameters are listed in Table 4.

Scenario A

In order to verify the effectiveness of the controller proposed above, the operating condition of expressway is chosen as a simulation scenario firstly, which is dry with an adhesion coefficient of 0.85, 40 and the

Table 3. The tire parameters.

Tire forces	В	С	D	E
F_{xf0} F_{xr0} F_{yf0} F_{yr0}	8.61	1.58	22,053	0.5624
	8.61	1.58	44,625	0.5624
	6.59	1.58	22,503	-0.3028
	6.59	1.58	44,625	-0.3028

Table 4. The control parameters.

Parameters	Value	Parameters	Value	Parameters	Value
C ₁ C ₄ σ ₃ k ₂ q r _{x2}	0.5 0.1 0.1 1 3/5 40	C ₂ σ ₁ σ ₄ η ₁ ρ r _V	0.1 0.4 5 0.5 3/5 40	c_3 σ_2 k_1 η_2 r_{x1} r_{y2}	0.6 0.05 0.05 35 35

maximum road curvature is 0.0025. Set a constant longitudinal velocity of the leading truck as $25\,\text{m/s}$, the initial longitudinal velocities of the following trucks as $23\,\text{m/s}$. Set the initial longitudinal spacing errors of the following trucks as $[2,3,4,5]\,\text{m}$, respectively. Both the initial lateral position errors and yaw angle errors are 0. Simulation results are shown in Figure 6(a) to (i).

Figure 6(a) shows the curvature variation of the expressway, where the maximum curvature is 0.0025. Figure 6(b) shows the driving paths of the truck

platoon on the expressway, where the four following trucks can travel along the desired trajectory. Figure 6(c) shows the phase trajectories of the following trucks. From Figure 6(c), the lateral velocities and the yaw rates of the four following trucks eventually converge to the origin. Figure 6(d) and (e) show the longitudinal velocities and longitudinal spacing errors of the truck platoon. Note that, the first following truck has the maximum overshoot of longitudinal spacing errors,

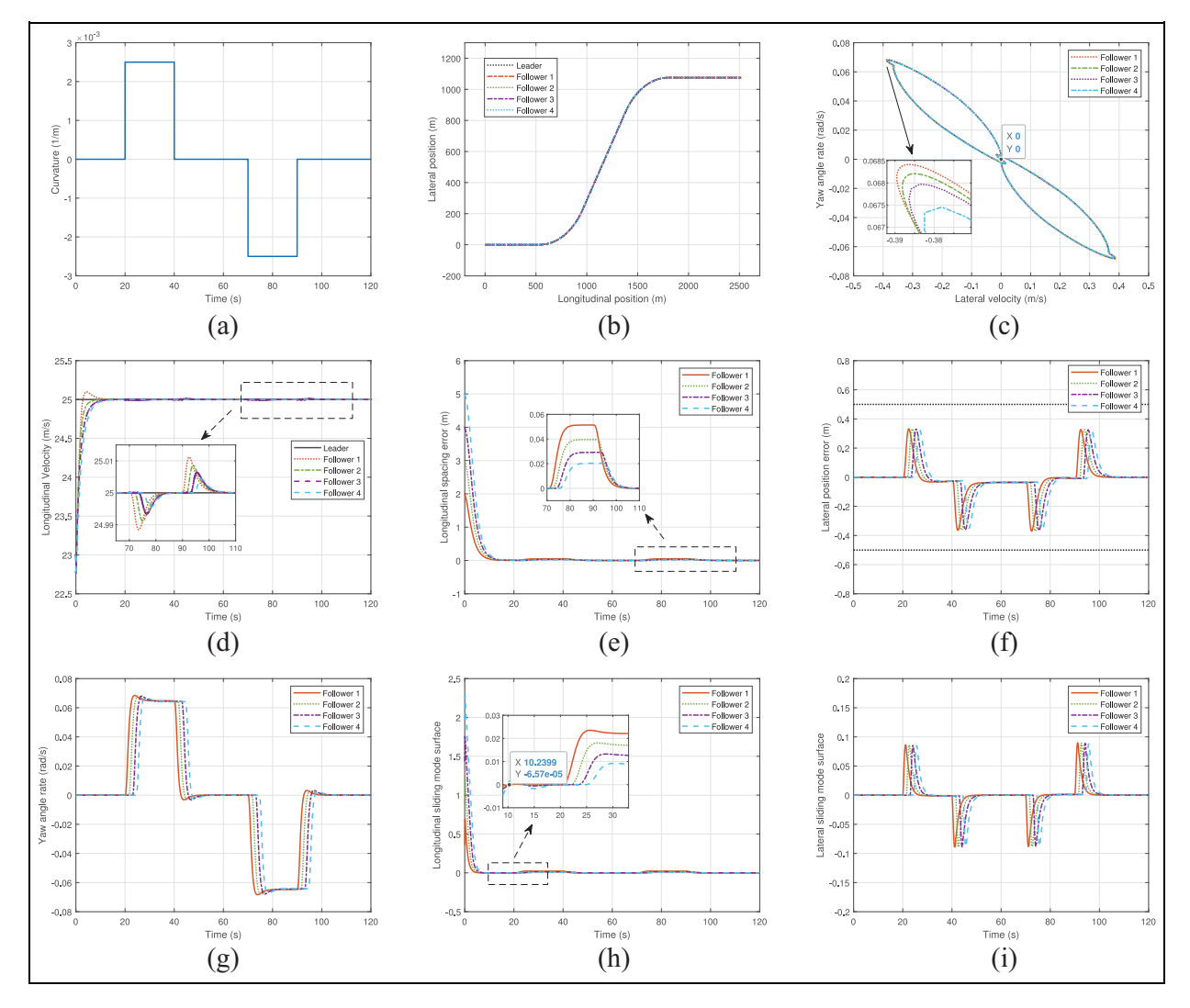


Figure 6. Truck platoon in scenario A: (a) road curvature, (b) driving paths, (c) phase trajectories, (d) longitudinal velocities, (e) longitudinal spacing errors, (f) lateral position errors, (g) yaw angle rate errors, (h) longitudinal sliding mode surfaces, and (i) lateral sliding mode surfaces.

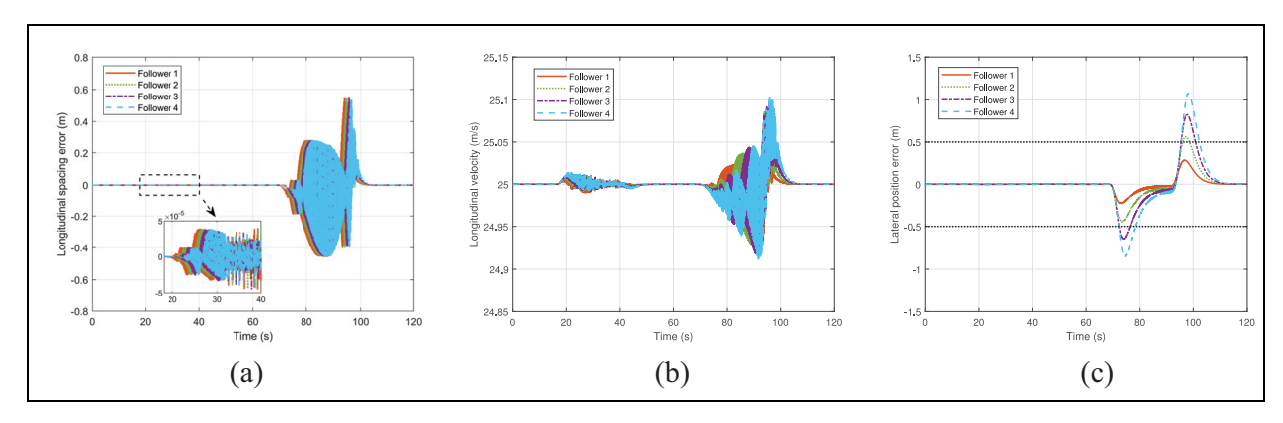


Figure 7. Truck platoon using kinematic model in scenario A: (a) longitudinal spacing errors, (b) longitudinal velocities, and (c) lateral position errors.

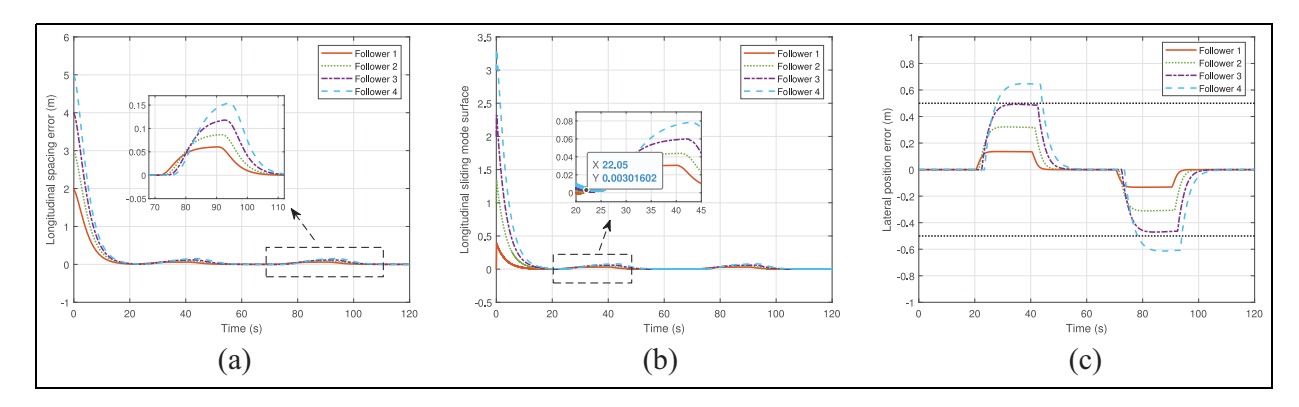


Figure 8. Truck platoon with the comparative controller in scenario A: (a) longitudinal spacing errors, (b) longitudinal sliding mode surfures, and (c) lateral position errors.

and the overshoot of the others are decreasing in order of the platoon, that is, the string stability of the truck platoon is guaranteed. Figure 6(f) and (g) show the lateral position errors and yaw angle rates of the following trucks. It can be found that the lateral position and yaw angle rates of the following trucks will change accordingly within an allowable range when the road curvature changes. Since the lateral position errors of following trucks are less than 0.5 m, the lateral constraint is satisfied. Figure 6(h) and (i) show the longitudinal and lateral sliding mode surfaces of the following trucks, in which the convergence time of longitudinal sliding surfaces is about 10.2 s.

Comparison Experiment A

In order to illustrate the necessity of using the dynamics model for truck platoons, a sliding mode controller with a classical kinematic model⁴¹ is chosen for comparison in this subsection. Set the constant longitudinal velocity of the truck platoon as 25 m/s, the initial longitudinal spacing errors of the following trucks as 0 m. The rest of the conditions are the same as in simulation scenario A and the controller parameters are shown in Table 4. The simulation results are shown in Figure 7(a) to (c).

Figure 7(a) and (b) show the longitudinal spacing errors and longitudinal sliding mode surfures of the following trucks. It can be seen that large oscillatory behaviors are caused when the truck platoon steers, which may lead to an instable movement of the truck platoon. Figure 7(c) shows the lateral position errors of the following trucks. The nonlinear characteristics of tires are not taken into account in the kinematic model, which might lead to the performance decaying. Furthermore, the lateral position of the following trucks travel beyond the lane boundary. Therefore, it is difficult to guarantee the safety of truck platoons at high speeds supposed that controllers are designed using the kinematic model (Figure 8).

Scenario B

In order to further verify the effectiveness of the proposed scheme, different road is chosen in this subsection. The road chosen can be described as

$$Y = 100\sin\left(\frac{X}{300}\pi\right) \tag{52}$$

where Y the lateral position and X is the longitudinal position.

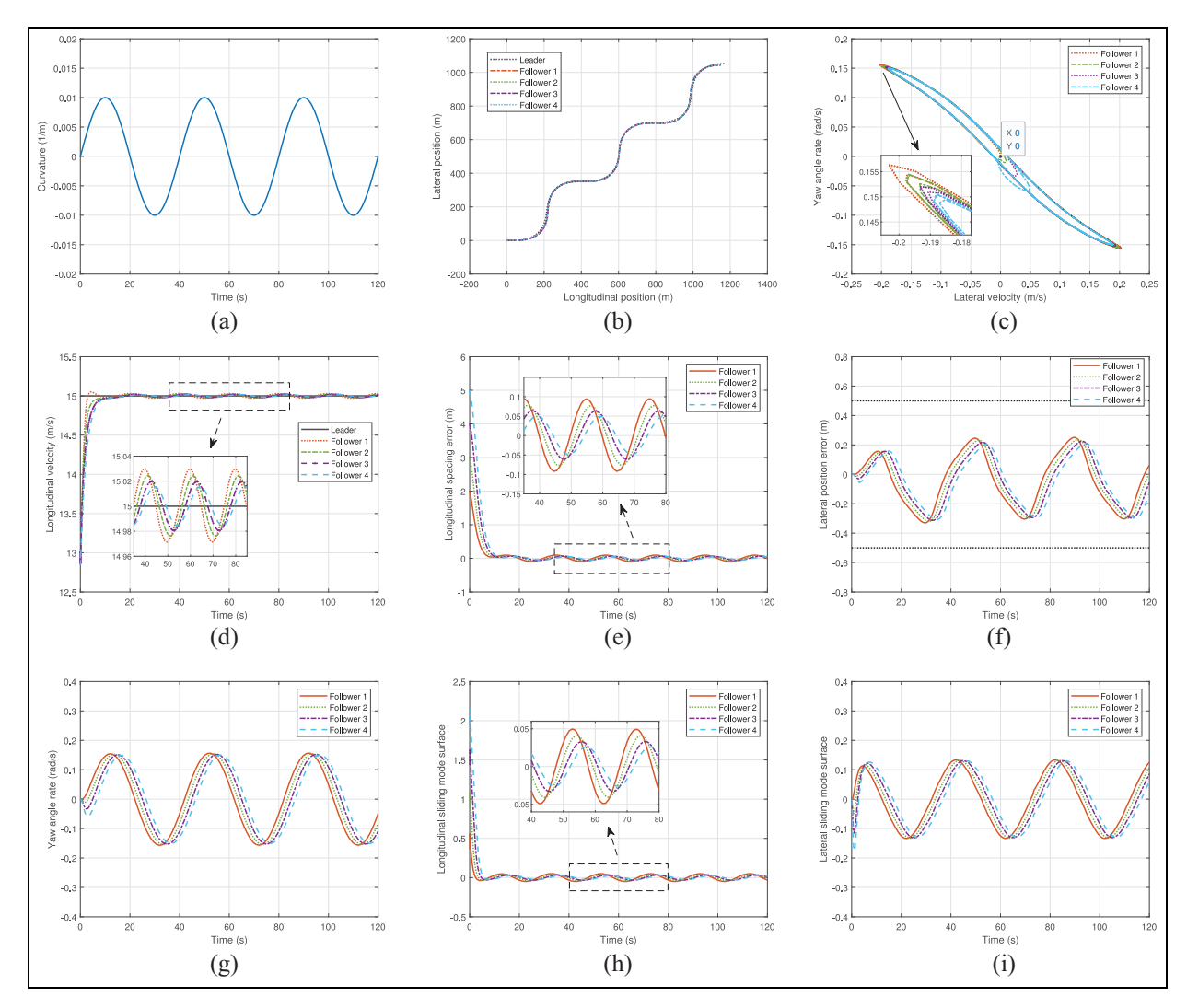


Figure 9. The truck platoon in scenario B: (a) road curvature, (b) driving paths, (c) phase trajectories, (d) longitudinal velocities, (e) longitudinal spacing errors, (f) lateral position errors, (g) yaw angle rate errors, (h) longitudinal sliding mode surfaces, and (i) lateral sliding mode surfaces.

The road curvature is

$$K = \frac{\left| \ddot{\mathbf{Y}} \right|}{\left(1 + \dot{\mathbf{Y}}^2 \right)^{1.5}} \tag{53}$$

In terms of (52) and (53), the road curvature is

$$K = 0.01 \sin\left(\frac{v_x}{300}\pi t\right) \tag{54}$$

Consider the road curvature as a bounded disturbance. Set the road adhesion coefficient as 0.85, 40 which is a dry road. The constant longitudinal velocity of leading truck is 15 m/s, the initial longitudinal velocities of the following trucks as 13 m/s. Set the initial longitudinal spacing errors of the following trucks as [2, 3, 4, 5] m, respectively. Both the initial lateral position errors and yaw angle errors are 0. The simulation results are shown in Figure 9(a) to (i).

Figure 9(a) shows the evolution of road curvature, where the maximum curvature is 0.01. Figure 9(b) is the traveling paths of the truck platoon on the road, which shows that four following trucks can travel along the desired trajectory. Figure 9(c) shows the phase trajectories of the following trucks, which shows that the phase trajectories of the following trucks do not cause large fluctuations under the disturbances caused by continuously change of curvature, that is, robustness of the truck platoon is demonstrated. Figure 9(d) and (e) show the longitudinal velocities and longitudinal spacing errors of the truck platoon. It can be found that the longitudinal velocities and longitudinal spacing errors of the following trucks will evolve accordingly within an allowable range when the road curvature continuously changes. Furthermore, the string stability of the truck platoon is demonstrated in Figure 9(e). Figure 9(f) and (g) show the lateral position errors and vaw angle rates of the following trucks, where the lateral position has a maximum error of about 0.3 m from

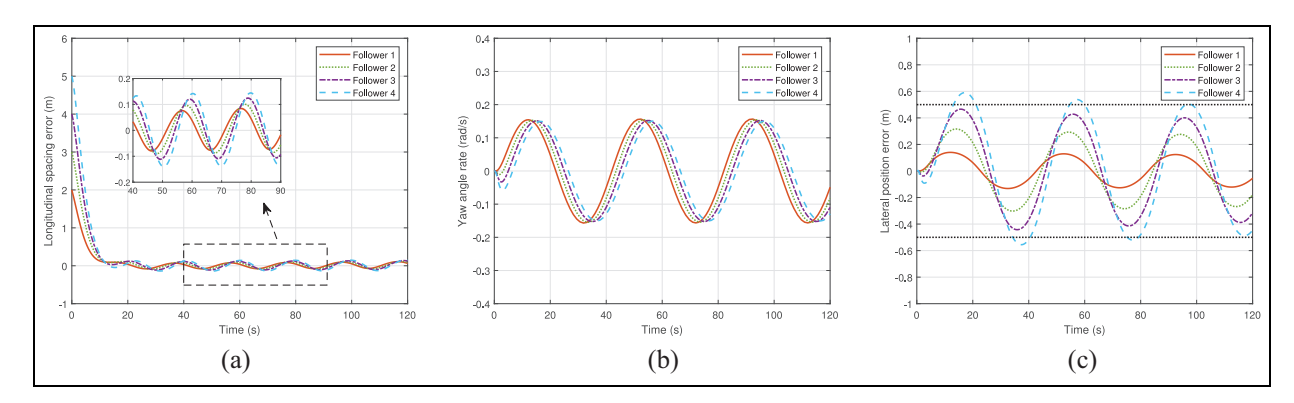


Figure 10. Truck platoon with the comparative controller in scenario B: (a) longitudinal spacing errors, (b) longitudinal sliding mode surfures, and (c) lateral position errors.

four following trucks to the centerline of the lane. Figure 9(h) and (i) show the longitudinal and lateral sliding mode surfaces of following trucks. It can be found that the steady state errors of the longitudinal sliding mode surfaces are about 0, which further illustrates the robustness of the proposed controller.

Comparison Experiment B

In order to compare the finite-time convergence of the proposed controller, a decoupled controller consisting of a longitudinal linear sliding mode controller³⁵ with the spacing policy of (8) and a lateral controller using PO driver model (Position and Orientation optimal preview driver model)²⁵ is chosen. In the simulation scenarios A and B, set the same initial conditions for the comparative controllers. The simulation results are shown in Figures 8 and 10.

Figures 8(a) and 10(a) show the longitudinal spacing errors of following trucks in scenario A and B. It can be found the forth following truck has the maximum overshoot of longitudinal spacing errors, and the overshoot of the others are decreasing in order of the platoon. Therefore, the controller designed with the spacing policy of (8) does not guarantee string stability of the truck platoon. Figures 8(b) and 10(b) show the longitudinal

sliding mode surfures of following trucks in scenario A and B. From Figure 8(b), it is shown that the convergence time of longitudinal sliding surfaces of four following trucks is about 22 s, which is much slower than the controller proposed in this paper. From Figure 10(b), it can be found that there is a little steady state error and chattering on the longitudinal sliding surfaces. Figures 8(c) and 10(c) show the lateral position errors of the four following trucks in scenario A and B. Since there is a little error in converting the road information into the information of the preceding truck when using the PO driver model is used, the lateral position errors will accumulate gradually. Therefore, when the number of trucks in platoon increases, the lateral position of the following trucks will cross the lane boundary, which might cause incidents.

Safety insurance of the truck platoon

In order to ensure the safety of the truck platoon, the maximum longitudinal velocity of the truck platoon needs to be investigated. Therefore, simulation experiments under different road curvatures and road adhesion coefficients are carried out in this subsection. The road curvatures of scenario A and B are chosen for simulation. Referring to Li et al.³⁸ and Hichri et al.,⁴⁰

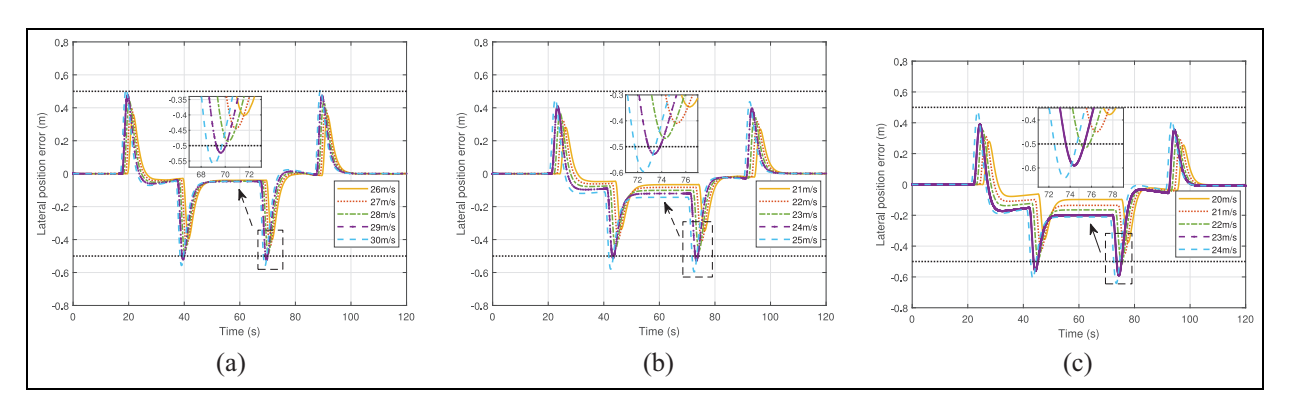


Figure 11. The lateral position errors of the first following truck in scenario A with three road adhesion coefficients: (a) $\mu = 0.85$, (b) $\mu = 0.60$, and (c) $\mu = 0.35$.

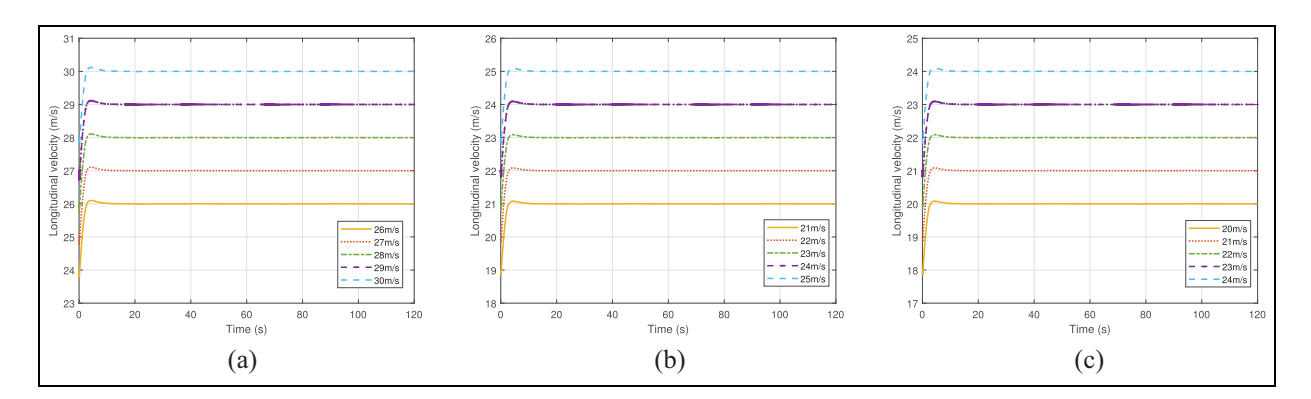


Figure 12. The longitudinal velocities of the first following truck in scenario A with three road adhesion coefficients: (a) $\mu = 0.85$, (b) $\mu = 0.60$, and (c) $\mu = 0.35$.

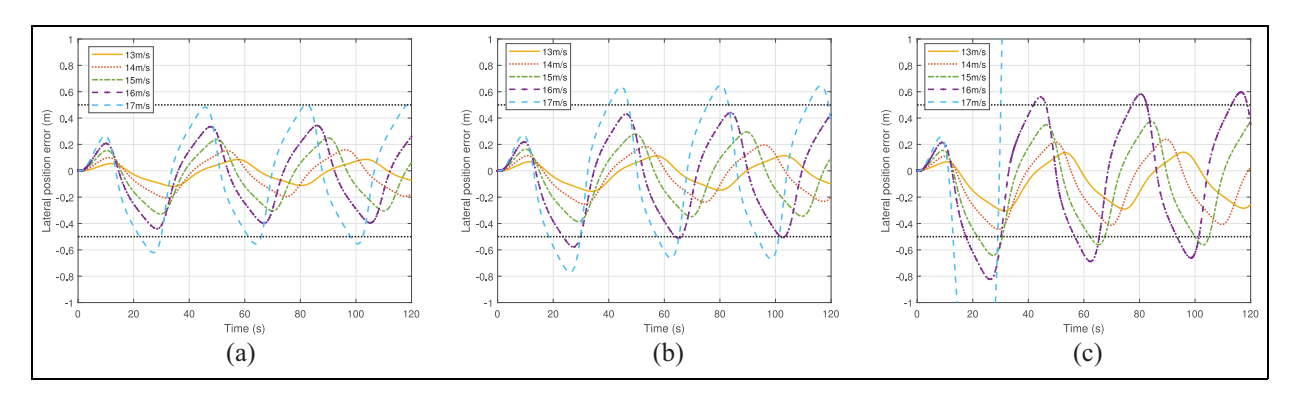


Figure 13. The lateral position errors of the first following truck in scenario B with three road adhesion coefficients: (a) $\mu = 0.85$, (b) $\mu = 0.60$, and (c) $\mu = 0.35$.

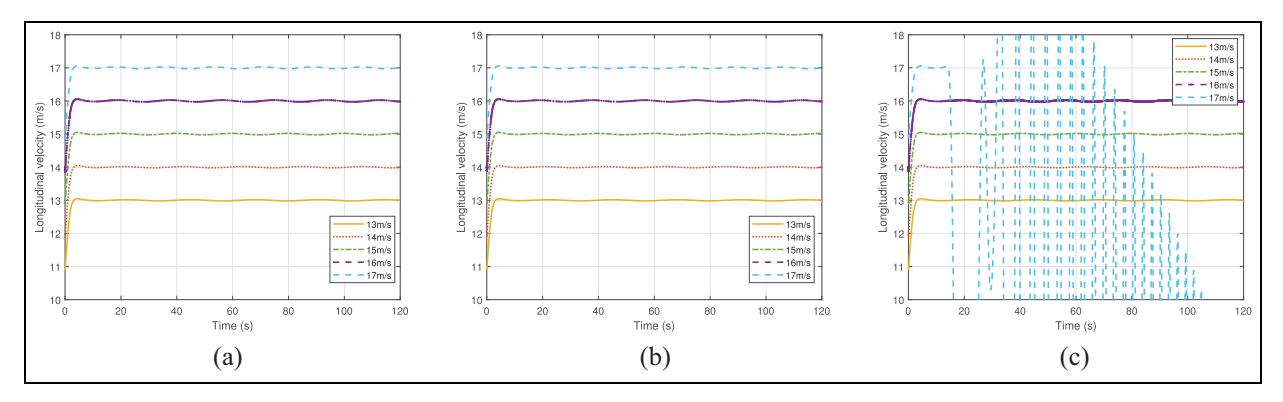


Figure 14. The longitudinal velocities of the first following truck in scenario B with three road adhesion coefficients: (a) μ = 0.85, (b) μ = 0.60, and (c) μ = 0.35.

the typical road adhesion coefficients are 0.85, 0.60, and 0.35. The errors of the first following truck in platoon is the largest one due to string stability, so the first following truck is chosen as comparison objective. Set the constant longitudinal velocity of the leading truck to be $2\,\mathrm{m/s}$ faster than the initial velocities of following trucks. Set the initial longitudinal errors of the following trucks as $2\,\mathrm{m}$, both the initial lateral position errors and yaw angle errors as 0. Whether the

lateral position of the following trucks cross the lane boundary is chosen as the criterion for judging the safety of truck platoon. The simulation results are shown in Figures 11 to 14.

Remark 6. Since the parameters of tires in the "Magic Formula" depend on the road adhesion coefficients, let $\mu = 1$ be nominal road adhesion coefficient, and $\mu = 0.35$ be wet road adhesion coefficient. The

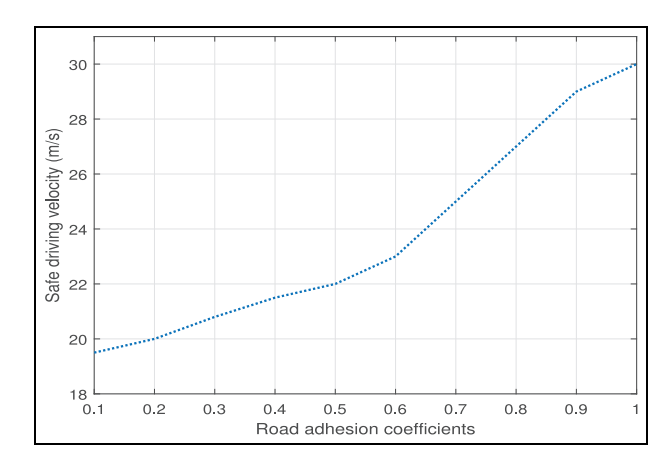


Figure 15. The maximum safe driving velocity of the truck platoon under different road adhesion coefficients and the road curvature of 0.0025.

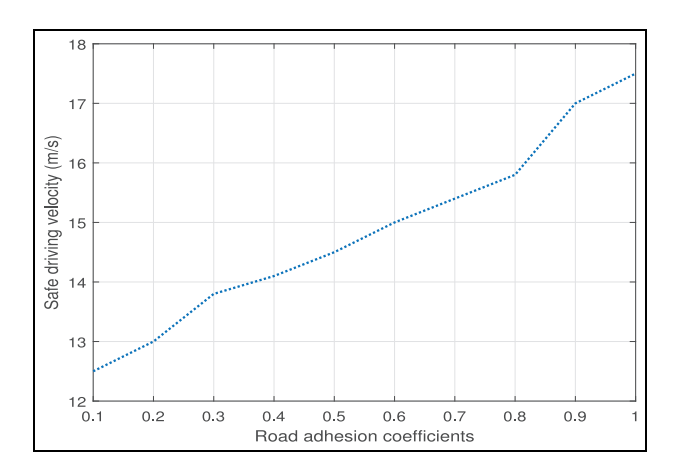


Figure 16. The maximum safe driving velocity of the truck platoon under different road adhesion coefficients and the road curvature of 0.01.

influence of the road adhesion coefficient on the tire forces in the "Magic Formula" is to change parameters B to $(2 - \mu)B$, C to $0.25 * (5 - \mu)C$, D to μD .

Figures 11 and 12 show the lateral position errors and longitudinal velocities of the first following truck under three road adhesion coefficients in scenario A, which show that the truck platoon can move stably with three road adhesion coefficients with the maximum road curvature of 0.0025. Among them, when $\mu = 0.85$, the maximum safe longitudinal velocity of the truck platoon is 28 m/s; when $\mu = 0.60$, the maximum safe longitudinal velocity is 23 m/s; when $\mu = 0.35$, the maximum safe longitudinal velocity is 21 m/s. It can be found that when the road adhesion coefficient decreases, the maximum safe longitudinal velocity of the truck platoon will also decrease accordingly. Therefore, through experiments conducted under different road adhesion conditions, if the longitudinal and lateral decoupling controllers are applied on the

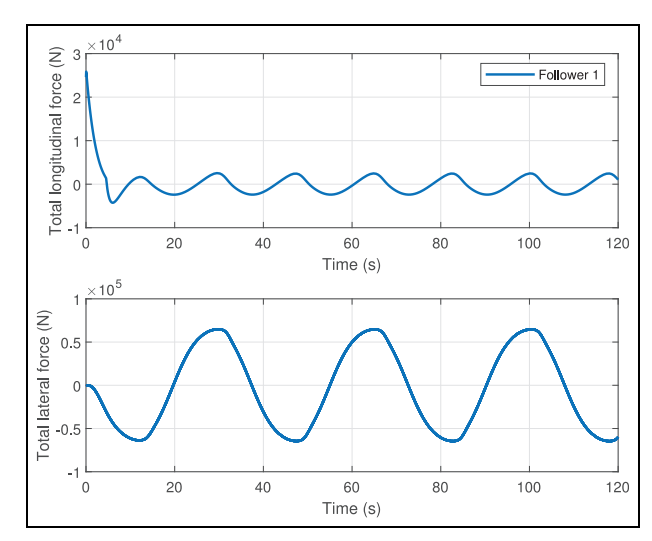


Figure 17. The total longitudinal and lateral forces of the first following truck under longitudinal velocity of 17 m/s and μ = 0.85.

expressway of the maximum road curvature of 0.0025, the maximum safe driving velocities of the truck platoon under different road adhesion coefficients are illustrated in Figure 15.

Remark 7. In this subsection, we have considered non-dry ground by varying the road adhesion coefficients. Figures 15 and 16 present the maximum safe velocities at different adhesion coefficients and curvatures.

Figures 13 and 14 show the lateral position errors and longitudinal velocities of the first following truck under three road adhesion coefficients in scenario B, which show that under the disturbances of continuously changing curvature, the truck platoon can move steadily. Among them, when $\mu = 0.85$, the maximum safe longitudinal velocity of the truck platoon is 16 m/s; when $\mu = 0.60$, the maximum safe longitudinal velocity is 15 m/s; when $\mu = 0.35$, the maximum safe longitudinal velocity is 14 m/s. Therefore, through experiments conducted under different road adhesion conditions, if the longitudinal and lateral decoupling controllers are applied on the expressway of the maximum road curvature of 0.01, the maximum safe driving velocities of the truck platoon under different road adhesion coefficients are illustrated in Figure 16.

From Figures 13(c) and 14(c), when the truck platoon is moving in scenario B with road adhesion coefficients of 0.35 at a longitudinal velocity of 17 m/s, the truck platoon occurs instable movements, that is, the truck platoon will be in danger.

Figure 17 shows the total longitudinal and lateral tire forces of the first following truck under longitudinal velocity of 17 m/s and road adhesion coefficients of 0.85. It can be found that the maximum longitudinal tire force of the truck platoon is about 25,000 N and

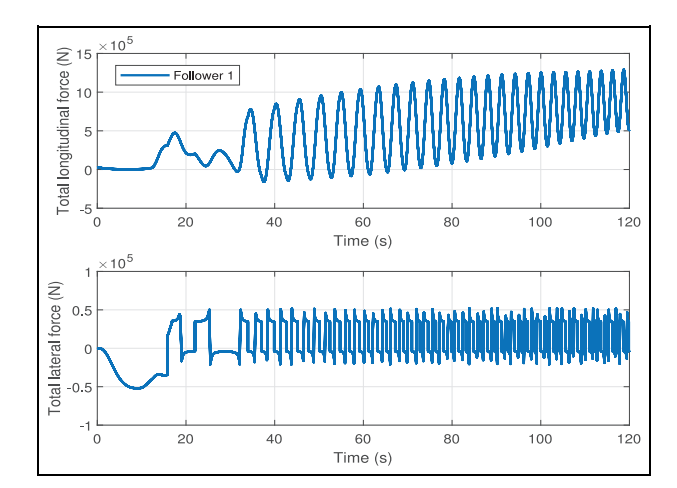


Figure 18. The total longitudinal and lateral forces of the first following truck under longitudinal velocity of 17 m/s and μ = 0.35.

the maximum lateral tire force is about 70,000 N. Considering the coupling characteristics of tire forces,³³ one has

$$\sqrt{F_{x,\max}^2 + F_{y,\max}^2} \leqslant \mu mg \tag{55}$$

Therefore, the maximum combined tire force does not reach its maximum restraint of the tire force, that is, the truck platoon do not occur instable movements, and the safety of the truck platoon will be guaranteed. On the contrary, Figure 18 shows that the total longitudinal and lateral tire forces of the first following truck under longitudinal velocity of 17 m/s and road adhesion coefficients of 0.35. From Figure 18, it can be calculated that the maximum combined tire force has already exceeded the maximum restraint of tire force. Therefore, the truck platoon will be unstable, and the safety of the truck platoon will not be guaranteed.

Conclusion

Aiming at fast convergence of errors of truck platoons, this paper proposed a distributed longitudinal and lateral control strategy based on finite-time sliding mode controller. Simultaneously, a second-order longitudinal platoon model and a lateral lane-keeping model were developed, in which a modified constant spacing policy to guarantee string stability was proposed, and both the finite-time stability and string stability of system of the truck platoon were analyzed. Moreover, co-simulation experiments were carried out on the joint simulation platform of Trucksim and Simulink, which showed that the proposed strategy can achieve fast convergence and string stability. Finally, in order to ensure the safe driving of the truck platoon, this paper gave the systematic estimation on the maximum driving velocity of the truck platoon under different working conditions consisting of road curvatures and road adhesion coefficients. The main reason for instability of truck platoon was analyzed. Therefore, the longitudinal and lateral control strategy proposed in this paper can guarantee the safety of truck platoons.

Note that the proposed finite-time convergence sliding mode controller induces chatter in the system, and fails to address the force constraints of longitudinal and lateral tires. Future works will focus on the two issues.

Declaration of conflicting interests

The author(s) declared no potential conflicts of interest with respect to the research, authorship, and/or publication of this article.

Funding

The author(s) disclosed receipt of the following financial support for the research, authorship, and/or publication of this article: This work is supported by the National Natural Science Foundation of China (No.62473167), the Natural Science Foundation of Jilin Province (No.20240402079GH), and the Foundation of Key Laboratory of Industrial Internet of Things and Networked Control (No.2019FF01).

ORCID iD

Shuyou Yu (b) https://orcid.org/0000-0002-3258-6494

References

- Liang KY, Mårtensson J and Johansson KH. Heavyduty vehicle platoon formation for fuel efficiency. *IEEE Trans Intell Transp Syst* 2015; 17(4): 1051–1061.
- Devika K and Subramanian SC. Sliding mode-based time-headway dynamics for heavy road vehicle platoon control. In: 2021 seventh Indian control conference (ICC), Mumbai, India, 20–22 December 2021, pp.265– 270. New York: IEEE.
- 3. Wu Y, Li SE, Cortés J, et al. Distributed sliding mode control for nonlinear heterogeneous platoon systems with positive definite topologies. *IEEE Trans Control Syst Technol* 2019; 28(4): 1272–1283.
- Lin F, Fardad M and Jovanovic MR. Optimal control of vehicular formations with nearest neighbor interactions. *IEEE Trans Autom Control* 2011; 57(9): 2203–2218.
- Fardad M, Lin F and Jovanović MR. Sparsity-promoting optimal control for a class of distributed systems. In: Proceedings of the 2011 American control conference, San Francisco, CA, USA, 29 June–1 July 2011, pp.2050– 2055. New York: IEEE.
- Lin F, Fardad M and Jovanović MR. Algorithms for leader selection in stochastically forced consensus networks. *IEEE Trans Autom Control* 2014; 59(7): 1789– 1802
- Peng B, Yu D, Zhou H, et al. A platoon control strategy for autonomous vehicles based on sliding-mode control theory. *IEEE Access* 2020; 8: 81776–81788.
- 8. Li Y, Lv Q, Zhu H, et al. Variable time headway policy based platoon control for heterogeneous connected

- vehicles with external disturbances. *IEEE Trans Intell Transp Syst* 2022; 23(11): 21190–21200.
- Hu M, Wang X, Bian Y, et al. Disturbance observerbased cooperative control of vehicle platoons subject to mismatched disturbance. *IEEE Trans Intell Veh* 2023; 8: 2748–2758.
- 10. Ali A, Garcia G and Martinet P. The flatbed platoon towing model for safe and dense platooning on highways. *IEEE Intell Transp Syst Mag* 2015; 7(1): 58–68.
- Zheng Y, Li SE, Li K, et al. Stability margin improvement of vehicular platoon considering undirected topology and asymmetric control. *IEEE Trans Control Syst Technol* 2015; 24(4): 1253–1265.
- Rajamani R. Vehicle dynamics and control. New York, NY: Springer Science & Business Media, 2011.
- Guo X, Wang J, Liao F, et al. Distributed adaptive sliding mode control strategy for vehicle-following systems with nonlinear acceleration uncertainties. *IEEE Trans* Veh Technol 2016; 66(2): 981–991.
- Guo G, Li P and Hao LY. A new quadratic spacing policy and adaptive fault-tolerant platooning with actuator saturation. *IEEE Trans Intell Transp Syst* 2020; 23(2): 1200–1212.
- Chen Q, Xu L, Zhou Y, et al. Finite time observer-based super-twisting sliding mode control for vehicle platoons with guaranteed strong string stability. *IET Intell Transp* Syst 2022; 16(12): 1726–1737.
- Naus GJ, Vugts RP, Ploeg J, et al. String-stable CACC design and experimental validation: a frequency-domain approach. *IEEE Trans Veh Technol* 2010; 59(9): 4268–4279.
- Weinstein AJ and Moore KL. Pose estimation of Ackerman steering vehicles for outdoors autonomous navigation. In: 2010 IEEE international conference on industrial technology, Via del Mar, Chile, 14–17 March 2010, pp.579–584. New York: IEEE.
- 18. Yu L, Bai Y, Kuang Z, et al. Intelligent bus platoon lateral and longitudinal control method based on finite-time sliding mode. *Sensors* 2022; 22(9): 3139.
- 19. Ali A, Garcia G and Martinet P. Minimizing the intervehicle distances of the time headway policy for urban platoon control with decoupled longitudinal and lateral control. In: *16th international IEEE conference on intelligent transportation systems (ITSC 2013)*, The Hague, Netherlands, 6–9 October 2013, pp.1805–1810. New York: IEEE.
- Dominguez S, Ali A, Garcia G, et al. Comparison of lateral controllers for autonomous vehicle: experimental results. In: 2016 IEEE 19th international conference on intelligent transportation systems (ITSC), Rio de Janeiro, Brazil, 1–4 November 2016, pp.1418–1423. New York: IEEE.
- 21. Bakker E, Pacejka HB and Lidner L. A new tire model with an application in vehicle dynamics studies. *SAE Trans* 1989; 98: 101–113.
- 22. Liu Y, Wei Y, Wang C, et al. Trajectory optimization for adaptive deformed wheels to overcome steps using an improved hybrid genetic algorithm and an adaptive particle swarm optimization. *Mathematics* 2024; 12(13): 2077.
- 23. Guo J, Li K and Luo Y. Coordinated control of autonomous four wheel drive electric vehicles for platooning

- and trajectory tracking using a hierarchical architecture. J Dyn Syst Meas Control 2015; 137(10): 101001.
- Feng G, Dang D and He Y. Robust coordinated control of nonlinear heterogeneous platoon interacted by uncertain topology. *IEEE Trans Intell Transp Syst* 2020; 23(6): 4982–4992.
- Shi S, Li L, Mu Y, et al. Stable headway prediction of vehicle platoon based on the 5-degree-of-freedom vehicle model. *Proc IMechE, Part D: J Automobile Engineering* 2019; 233(6): 1570–1585.
- Li Y, Tang C, Peeta S, et al. Integral-sliding-mode braking control for a connected vehicle platoon: theory and application. *IEEE Trans Ind Electron* 2018; 66(6): 4618–4628.
- Cao Y and Ren W. Finite-time consensus for multi-agent networks with unknown inherent nonlinear dynamics. *Automatica* 2014; 50(10): 2648–2656.
- Kwon JW and Chwa D. Adaptive bidirectional platoon control using a coupled sliding mode control method. *IEEE Trans Intell Transp Syst* 2014; 15(5): 2040–2048.
- 29. Yu S, Sheng E, Zhang Y, et al. Efficient nonlinear model predictive control of automated vehicles. *Mathematics* 2022; 10(21): 4163.
- 30. Wang X, Shi S, Liu L, et al. Analysis of driving mode effect on vehicle stability. *Int J Automot Technol* 2013; 14: 363–373.
- 31. Sugimachi T, Fukao T, Suzuki Y, et al. Development of autonomous platooning system for heavy-duty trucks. *IFAC Proc Vol* 2013; 46(21): 52–57.
- 32. Pacejka HB and Bakker E. The magic formula tyre model. *Veh Syst Dyn* 1992; 21(S1): 1–18.
- 33. Pacejka HB. *Tire and Vehicle Dynamics*. 3rd ed. Oxford: Butterworth-Heinemann, 2012.
- 34. Ko Y and Song C. Vehicle modeling with nonlinear tires for vehicle stability analysis. *Int J Automot Technol* 2010; 11(3): 339
- Bom J, Thuilot B, Marmoiton F, et al. A global control strategy for urban vehicles platooning relying on nonlinear decoupling laws. In: 2005 IEEE/RSJ international conference on intelligent robots and systems, Edmonton, AB, Canada, 2–6 August 2005, pp.2875–2880. New York:
- Menzel T, Bagschik G and Maurer M. Scenarios for development, test and validation of automated vehicles. In: 2018 IEEE intelligent vehicles symposium (IV), Changshu, China, 26–30 June 2018, pp.1821–1827. New York: IEEE.
- Swaroop D. String stability of interconnected systems: an application to platooning in automated highway systems. Berkeley, CA: University of California, 1994.
- 38. Li L, Wang FY and Zhou Q. Integrated longitudinal and lateral tire/road friction modeling and monitoring for vehicle motion control. *IEEE Trans Intell Transp Syst* 2006; 7(1): 1–19.
- Shen Y and Huang Y. Uniformly observable and globally lipschitzian nonlinear systems admit global finitetime observers. *IEEE Trans Autom Control* 2009; 54(11): 2621–2625.
- 40. Hichri Y, Cerezo V and Do M. Friction on road surfaces contaminated by fine particles: some new experimental

- evidences. *Proc IMechE*, *Part J: J Engineering Tribology* 2017; 231(9): 1209–1225.
- 41. Samson C. Control of chained systems application to path following and time-varying point-stabilization of
- mobile robots. *IEEE Trans Autom Control* 1995; 40(1): 64–77
- 42. Mammar S and Koenig D. Vehicle handling improvement by active steering. *Veh Syst Dyn* 2002; 38(3): 211–242.